OPEN ACCESS

University of BRISTOL

Imani Asrai, R., Newman, S. T., & Nassehi, A. (2018). A mechanistic model of energy consumption in milling. *International Journal of Production Research*, *56*(1-2), 642-659. https://doi.org/10.1080/00207543.2017.1404160

Peer reviewed version

Link to published version (if available):
10.1080/00207543.2017.1404160

Link to publication record in Explore Bristol Research
PDF-document

This is the author accepted manuscript (AAM). The final published version (version of record) is available online via Taylor and Francis at http://www.tandfonline.com/doi/full/10.1080/00207543.2017.1404160 .Please refer to any applicable terms of use of the publisher.

University of Bristol - Explore Bristol Research
General rights

This document is made available in accordance with publisher policies. Please cite only the published version using the reference above. Full terms of use are available:
http://www.bristol.ac.uk/red/research-policy/pure/user-guides/ebr-terms/

A mechanistic model of energy consumption in milling

Reza Imani Asrai[a]*, Stephen T Newman[a], Aydin Nassehi[b]

a: Department of Mechanical Engineering, University of Bath, Bath, UK
b: Faculty of Engineering, Bristol University, Bristol, UK

**: r.imani.asrai@bath.ac.uk*

Abstract

In this paper, a novel mechanistic model is proposed and validated for the consumption of energy in milling processes. The milling machine is considered as a thermodynamic system. Mechanisms of the significant energy conversion processes within the system are used to construct an explicit expression for the power consumption of the machine as a function of the cutting parameters. This model has been validated experimentally and is shown to be significantly more accurate than popular existing models. A simplified form of the model is also proposed that provides a balance between complexity and accuracy.

The novelty of the model is that it maps the flow of energy within a machine tool, based solely on the active mechanisms of energy conversion. As a result, only limited assumptions are made in the model, resulting in an error of less than one percent, verified by experiments. This accurate model can be used to substantially reduce energy consumption in milling processes at machine and factory levels leading to massive cost savings and reduction of environmental impact of numerous industries. The generality of the modelling method makes it applicable to other types of machine tools with minimal adjustments.

Keywords:

Energy Efficient Manufacturing, Green manufacturing, Machine Tools, Process modelling, Energy modelling,

1. Introduction to energy consumption in machine tools

Strategies for sustainable development involve three major technological changes: energy saving on the demand side, efficiency improvements in energy production and replacement of fossil fuels by various sources of renewable energy (Lund, H. 2007). Energy-efficient utilisation of end users of energy is a low-cost and flexible approach towards energy saving on the demand side. Machine tools are end users of electrical energy.

The total rate of energy consumption of machine tools at global or national levels were not found in the authors' search of statistics. US Energy Information Administration (2016, p.113) classifies industries, according to their global energy consumption, into three classes: *energy-intensive manufacturing*, *non-energy-intensive manufacturing* and *non-manufacturing*. There are seven subclasses in the *energy-intensive manufacturing*, but the *fabricated metal products* is listed under one of the two subclasses of the *non-energy-intensive manufacturing*. So the cumulative energy consumption of machine tools, which is a fraction of the energy consumption of the *fabricated metal products* industry, cannot be larger than two order of magnitude smaller than the total industrial consumption. As a response to the aforementioned lack of specific data, Rajemi et al. (2010) suggested that as metal fabrication contributes to *mechanical engineering* sector, the total energy consumed by machine tools in 2008 must be a part of that sector's energy consumption of 8TWh. The *industrial electricity consumption* was 342TWh that year.

In 2016, the total energy consumption in the UK exceeded 140.7Mtoe, i.e. million tonnes of oil equivalent. The industrial use accounted for 23.7Mtoe of it, of which, 7.9Mtoe, was consumed in the form of electricity (Department for Business, Energy & Industrial Strategy, 2017a, pp.29-30). Among the processes that constitute the industrial energy consumption, the *manufacture of fabricated metal products, except machinery and equipment* consumed 654ktoe, of which 321ktoe was consumed in the form of electricity (Department for Business, Energy & Industrial Strategy, 2017b, Table 4.04). 147ktoe of this electricity is consumed in low temperature processes. Machine tools receive their energy input as electricity and perform low temperature processes. Machining of metals is thus one of the energy consuming processes that constitute the aforementioned 147ktoe. So, the overall energy consumed for machining

of metal parts in the UK during 2015, is a fraction of 147ktoe. This, provides an upper limit for the total energy consumed by machine tools in the UK during 2016 for machining metals.

$$E_{Machining-2016} < 147ktoe \quad (1)$$

147ktoe is equivalent to 1.7TWh, in contrast with the 8TWh upper bound suggested by Rajemi et al. (2010). This upper limit is equal to 1.9% of the industrial electricity consumption, 0.6% of the industrial energy consumption, and 0.1% of the total energy consumption of the UK (Department for Business, Energy & Industrial Strategy, 2017b). So, the energy consumption of machine tools is not among the major energy consuming industrial processes in the UK, but assuming that the fraction of the above 147ktoes that corresponds to machining processes is not more than one order of magnitude smaller than 1, then $E_{Machining-2016}$ can be estimated to be within the range [10,10^2] ktoe, equivalent to [0.1,1] TWh of electricity, and equal to about [0.1-1] percent of the industrial electricity consumption in the UK. In monetary terms, at 20p/kWh, that is equivalent to £[20,200]m per annum, or O(£10^2m/a). This is the order of magnitude of the cost incurred annually to the manufacturing industry in the UK, due to its consumption of electrical energy in machining processes. So, it is expected that 1% improvement in the energy efficiency of the machining processes in the UK, to be equivalent to a cost reduction of the order of magnitude of £1m.

Energy is consumed in all four stages of a machine tool's life-cycle; manufacturing, transportation, use and end-of-life. Dematerialisation of machine tools can reduce the energy consumed during all four stages. For the use stage, the study of energy consumption has been ongoing since the early 1980s, when De Filippi et al. (1981) noticed a trend in fitting NC machine tools with increasingly powerful motors, caused by a clear request from the customers, in the few years prior to the publication of their work and raised the question whether that demand reflected the existence of a real need. They found that the installed power of machine tools is never fully exploited. They also found that the mass of machine tools is an increasing function of their installed power and concluded that increasing installed power of a machine tool is likely to result in an unnecessary rise in its cost. Lack of priority for energy efficiency among machine tool manufacturers has left potential for improvement of up to a factor of 3 through redesign of machine tools (Duflou et al., 2012). Process level hardware enhancement approaches have also been proposed to reduce energy consumption during machining. For example,

using diamond-like tools can reduce energy consumption by up to 36% (Zolgharni et al., 2008).

In addition to hardware improvement methods, optimal utilisation of the existing machine tools can significantly improve their energy efficiency. At factory level, Su et al. (2017) used an integrated model to minimise energy consumption, while maintaining desired productivity in Bernoulli serial lines. Mouzon et al. (2010), noting the fact that a significant amount of energy saving is possible by turning off underutilised machines, proposed several dispatching rules in order to increase the energy efficiency at factory level.

At machine level, Li et al. (2013) proposed a framework for characterising energy consumption of machining manufacturing systems based on a hierarchical description of the holistic energy flow in machining manufacturing systems in three layers of machine tool, task and auxiliary production. They also classified quantitative energy consumption models at system level into models in spatial and temporal dimensions. This framework provides a robust basis for breakdown of energy consumption in machining manufacturing systems into a number of simple cases, each dealing a certain layer, at a certain space and time interval. Hu et al. (2017) investigated optimisation of energy usage by sequencing manufacturing features.

Optimisation of process parameters can allow reduction in energy consumption to a factor of 1.1, i.e. 10% increase (Duflou et al., 2012). Identifying the optimum process parameters for the purpose of energy efficiency improvement would require information about the behaviour of a machine tools' energy consumption as a function of the controllable process parameters. Prabhu et al. (2017) identifies modelling energy consumption in varying scales and subsystems as one of the three ley challenges in energy-aware manufacturing operations, along with the balance between energy efficiency and manufacturing-system effectiveness and the volatility in energy availability, supply and cost.

The aim of this research is thus to construct a model that represents the consumption of energy in a typical CNC machine tool during the milling process and to provide a predictive formula for the power consumption of the machine tool as a function of milling process parameters. This paper presents a more general form of the approach presented in one of the authors' PhD thesis (Imani Asrai, 2013) to mechanistic

modelling of energy consumption in a milling machines. The experimental data used in this paper for validation of the constructed model is also taken from the aforementioned thesis, where further details of the data and the data acquisition process can be accessed.

The structure of this paper thus consists of this section as background. In section 2, a review of the literature on energy consumption models for machine tools is presented and a gap is identified for sufficiently precise mechanistic model at machine level. One such model is constructed in section 3, based on the energy conversion mechanisms in a typical CNC machine tool. In section 4, the constructed model is verified for the case of steady-state slot milling of Al 6082 on a 3-axis CNC milling machine with 14mm carbide-steel end mill. Section 5 discusses the superior accuracy of the model in comparison to a number of existing model and presents a simplified form of the model. The final section outlines the conclusions and possible avenues for future work.

2. Literature review: energy consumption models for machine tools

Akbari et al. (2001) noticed that during cutting processes, the power consumption of the peripheral equipment, e.g. coolant pump, hydraulic pump and control devices, is usually higher than power consumed directly for cutting. They argued that it is possible to significantly reduce the energy consumption during machining through dry cutting and increasing the process speed. The former turns off a major energy consumer component of the machine tool and the latter reduces the process time, hence smaller time integral of the peripherals' power, i.e. their energy consumption during the process. Dahmus and Gutowski (2004) observed a trend towards fitting more auxiliary equipment on machine tools, that could potentially lead to lower energy efficiency. Their analysis of energy consumption in a number of machine tools showed that the maximum share of electric power used directly for cutting can be as small as 14.8% in the case of a large machining centre, in contrast with up to 69.4% in the case of a manual milling machine. They also concluded that the energy consumption of machine tools could be broken down into a combination of some constant terms that do not depend on the material removal process and a variable part that is a result of material removal and depends on cutting process parameters. The variable part was found to increase by the increase in the rate of the Material Removal Rate (MRR). The observation that a machine tool's power consumption is almost constant when it is not cutting material

has led to models which are based on defining different states of function for a machine tool and assigning a constant power consumption to each state, except for the cutting state. For example, Balogun and Mativenga (2012) defined three different states: Basic, Ready and Cutting, and assumed constant power consumption for states other than Cutting. Since the desirable function of a machine tool takes place during the cutting process, then minimising the time that a machine spends in other states, is a simple way of improving its energy efficiency. Energy-aware scheduling is an example of efforts towards harnessing this potential (Bruzzone et al. 2012).

The strictly increasing relation between the MRR, and energy efficiency of machining processes was further emphasised in Diaz et al. (2009). They initially hypothesised the existence of an optimum MRR, above and below which, the efficiency to fall. However, in their experiments, they found that the optimum MRR, is larger than the physical limitations of the cutting process allow, and all their experimental results show a strictly increasing relation between the MRR and the energy efficiency of the cutting process, suggesting that the highest efficiency may be achieved at highest possible MRR.

Empirical and mechanistic models have been developed for finding quantitative expression of energy consumption in machine tools in terms of process parameters. Draganescu et al. (2003) applied Response Surface Methodology for empirical modelling of energy consumption of a milling machine. Their model states energy efficiency in terms of spindle speed and spindle torque. Since the latter is not a controllable operation parameter, this model cannot be directly used as an instrument for optimisation of energy consumption in machining operations.

Gutowski et al. (2006) proposed that the variable part of power is proportional to the MRR. Equation 2.a expresses their model, in which, P represents machine tool's overall power consumption, P_0, the constant term and k, a constant coefficient.

$$P = P_0 + k(MRR) \tag{2.a}$$

Dividing both sides of the above equation by MRR gives an equivalent form of it, equation 2.b, which appears frequently in the literature. In this equation, SEC is the Specific Energy Consumption and C_0 and C_1 are constant coefficients to be evaluated experimentally.

$$SEC = C_0 + \frac{C_1}{MRR} \tag{2.b}$$

Since its introduction, equation 2, has been used extensively for modelling the power

consumption of machine tools during cutting operations. Imani Asrai et al (2009) provided a process level model of energy consumption and Li and Kara (2011) used it to model energy consumption in a turning machine and found out that it can predict the machine's power with 90% accuracy. Kara and Li (2011) extended their work to include eight different machine tools and considering both wet and dry cutting. Diaz et al. (2011) decomposed a milling machine's energy consumption to a cutting power that is modelled by equation 2 and an air cutting power, which is assumed to be constant. Rajemi et al. (2010) and Mori et al. (2011) used similar decompositions of the process time and used equivalents of equation 2 to predict energy consumption during cutting time, while assuming different constant powers for other states of machine operation. Jeon et al. (2017) used equation 2 in their study of power demand risk models on milling machines.

Equation 2 suggests that regardless of the individual cutting parameters, power consumption should remain unchanged as long as the MRR is kept constant. However, experimental data have revealed that this is not necessarily the case and the error in this statement can be considerably large. Newman et al. (2012) observed that in the case of slot milling aluminium alloy 6042 at constant MRR and variable depths of cut the change in power consumption could be up to 13 percent. Camposeco-Negrete (2013) also reported considerable disparity in energy consumption at constant MRR and variable spindle speeds. Liu et al. (2015) point at the inaccuracy of equation 2 in predicting energy consumption during finish hard milling of tool steel. This indicates the requirement for more precise models. Modified forms of equation 2 have been proposed to increase its accuracy. Li et al. (2013) incorporated the effect of spindle rotation in energy consumption by adding a linear function of spindle speed to equation to reach:

$$SEC = C_0 + C_1\left(\frac{1}{MRR}\right) + C_2\left(\frac{n}{MRR}\right) \quad (3)$$

Guo et al. (2012) modified equation 2 for turning processes, by considering a nonlinear relationship between the variable part of power and process parameters:

$$SEC = C_0 \cdot v_c^{\alpha} \cdot f^{\beta} \cdot a_p^{\gamma} \cdot D^{\varphi} + \frac{C_1}{v_c \cdot f \cdot a_p} \quad (4)$$

Where: v_c is the cutting speed, f is the feed rate, a_p is the depth of cut and D is the final workpiece diameter. The constant coefficients and powers are to be evaluated

experimentally. Hu et al. (2014) use a similar model to predict the energy consumption in turning processes.

Many models have been developed for energy consumption at the process level. Munoz and Sheng (1995) constructed a model based on the mechanics of chip formation. Kishawy et al. (2004) decomposed the process energy into three parts: the energy for plastic deformation in the primary and secondary shear zones, E_P and E_S, and the energy for debonding the particle from the matrix, E_D. They used mechanistic and empirical models for each of the three and constructed a model for energy consumption at process level by adding up the three models. Wang et al. (2017) categorised the process time into setup time, T_S, cutter engagement time, T_{ce}, cutting time, T_c, cutter retract time, T_{cr}, tool exchange time, T_{te}. They used an existing force model to directly evaluate energy consumption during the process.

Tool wear affects the energy consumption of metal cutting processes and models have been developed to incorporate this effect. As an example, Yoon et al. (2014) proposed the effect of tool wear as an additional term to the power:

$$P_{machining} = f_1(n, f, a_p) + f_2(n, f, a_p)V_B \quad (5)$$

Where: n, f, a_p and VB are spindle speed, feed rate, depth of cut and the tool's flank wear, respectively. f_1 and f_2 are second order functions of n, f and a_p with interactions.

To summarise, the existing models for energy consumption in machine tools can be roughly categorised into three types (Cai et al., 2017): linear models in terms of MRR, detailed parameter models and process oriented models. The conducted review of literature shows that although there are mechanistic models of energy consumption in machine tools at process level, there is currently no such model at machine level. There exist empirical models, but they either lack precision in predicting the actual energy consumption, or contain many coefficients that need to be evaluated for each specific combination of machine tool, cutting tool, workpiece material, etc.

3. A model for energy consumption of a CNC milling machine

This paper aims to provide a mechanistic model, based on the energy conversion mechanisms within a typical machine tool.

3.1. CNC machine tool as a thermodynamic system S

Consider a CNC milling machine as a thermodynamic system S, in an environment at temperature T_0 as shown in figure 1. Assume there is no mass exchange between S and its environment. S receives energy from the power grid in electromagnetic form, through the machine's electric plug conductors, at the rate of $P(t)$. The input energy experiences a number of conversions before leaving S for the environment. S surrenders energy to the environment in thermal form at the rate of $\dot{Q}_{out}(t)$, and in mechanical form, through sound and vibration, at the rate of $\dot{E}_{Mout}(t)$. According to the 1st law of thermodynamics, during the infinitesimal time interval $[t, t + dt]$:

$$dQ = dW + dU \tag{6}$$

where: dQ is the infinitesimal heat entered S, dW is the infinitesimal work performed by S on the environment and dU is the infinitesimal increase in the internal energy of S. By definition of $\dot{Q}_{out}$:

$$dQ = -\dot{Q}_{out}\mathrm{d}t \tag{7.a}$$

dW is the sum of electromagnetic and mechanical work performed the by S on the environment, including G. By definitions of P and $\dot{E}_{Mout}$:

$$dW = -Pdt + \dot{E}_{Mout}dt \tag{7.b}$$

Replacing dQ and dW in equation 6 by their equivalents from equation 7:

$$P = \dot{Q}_{out} + \dot{E}_{Mout} + \frac{dU}{dt} \tag{8}$$

The internal energy of S, $U(t)$, can be partitioned, as a set, according to form, into U_E, U_M, U_T, U_C and U_N, respectively for Electromagnetic, Mechanical, Thermal (including radiation), Chemical and Nuclear. Normally, within a machine tool, the rates of energy conversion due to nuclear and chemical reactions are very much smaller than the total input power, P. Therefore, U_N and U_C have been assumed constant in this paper and the flows of energy into and out of them have been neglected when mapping energy flows. So the only significant conversions take place between electromagnetic, mechanical and thermal forms. Therefore:

$$U = U_E + U_M + U_T + cte \tag{9}$$

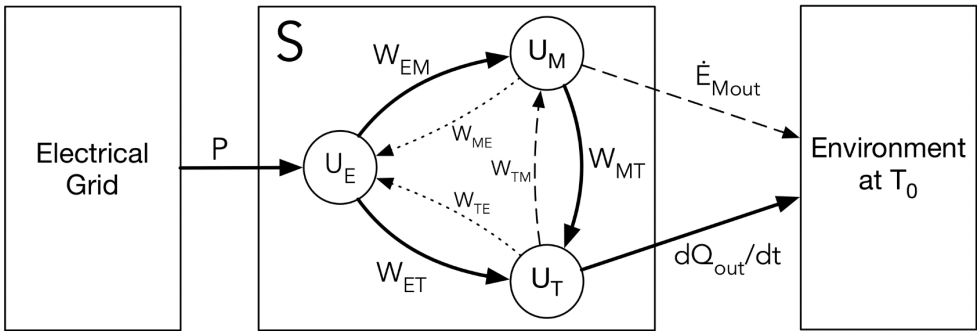

Figure 1. A CNC milling machine as a thermodynamic system, S

In figure 1, the curved arrows, represent the conversions of energy between forms within S. W_{ij} represents the rate of conversion from form i to form j, e.g. W_{EM} represents the rate of conversion from Electrical form to Mechanical. There are 6 possible direct conversions between U_E, U_M and U_T. The rates of 2 of them, W_{TE} and W_{ME}, shown by dotted curved arrows in figure 1, are zero. There is no direct mechanism of active energy conversion from thermal form to electromagnetic, e.g. thermoelectric, within a typical CNC machine tool. Neither is a mechanism of conversion from mechanical to electromagnetic, as long as the average values of quantities over one or many AC cycles are considered. So:

$$W_{TE} = 0 \quad (10.a)$$
$$W_{ME} = 0 \quad (10.b)$$

The rate of conversion from thermal to mechanical, W_{TM}, shown by dashed curved arrow, is also very small in comparison to the rate of opposite conversion, W_{MT}. Thermal engines convert thermal energy to mechanical. The efficiency of thermal engines is limited to the Carnot efficiency. In the volume of S, only within a small neighbourhood of the tool-workpiece contact is the temperature high enough, so the Carnot is not negligible compared to 1. In this region, a fraction of the input mechanical energy, which itself is a fraction of W_{EM}, converts to high temperature heat. If the cutting process is carried out with coolant, then almost all of the high temperature heat converts to low temperature heat, before any of it reaches a thermal engine. Even if the machining is performed without coolant, most of the high temperature heat is dissipated to low temperature heat, through thermal conduction and radiation, and only the remaining fraction of it is available to thermal engines. Normally, there is no thermal engine for energy recovery installed on CNC machines. The only existing thermal engine within S is natural convection which has a much lower than Carnot efficiency.

Therefore, the rate of conversion from thermal to mechanical is negligible in comparison with W_{MT}.

$$W_{TM} \ll W_{MT} \tag{11.a}$$

$\dot{E}_{Mout}$, The rate of output energy in the mechanical form as sound and vibration, shown with a dashed straight arrow, is very small, compared to other terms in the above equation. For example, if the sound intensity just outside the surface of the machine tool is as high as 100dB, the total power of the output acoustic wave is of the order of magnitude of 10^{-1}W, considering an outer surface area of the order of magnitude of $10m^2$ for the machine. This is 4 orders of magnitude smaller than the idle power of a typical CNC machine tool, which is of the order of magnitude of kilowatts. Therefore:

$$\dot{E}_{Mout} \ll W_{EM} \tag{11.b}$$

The three remaining conversion rates, W_{EM}, W_{ET} and W_{MT} are not necessarily negligible. Writing the conservation of energy for the subset U_T and applying 11.a results in:

$$W_{MT} + W_{ET} \approx \frac{dU_T}{dt} + \dot{Q}_{out} \tag{12}$$

Incorporating equations 12 and 9 into 8 and applying 11.b:

$$P \approx W_{MT} + W_{ET} + \frac{dU_M}{dt} + \frac{dU_E}{dt} \tag{13}$$

Equation 13 always holds, irrespective of the process. The uncertainty is because of 11.a and 11.b, and its relative scale is estimated to be no more than 10^{-3}. Equation 13 has been used in this paper to construct a quantitative model of P in terms of process parameters, through mechanistic models of the terms on the right side of the equation, for the specific case of steady-state slot milling.

3.2. Steady-state slot milling

Imagine the machine during a steady-state slot cutting. In steady-state, at every point in S, the temperature, velocity, material properties and electromagnetic field are constant. So, the densities of thermal and electromagnetic internal energies are constant. So their volume integrals over S are constant.

$$\frac{dU_E}{dt} = 0 \tag{14}$$

The internal mechanical energy U_M is the sum of kinetic and potential energies U_K and U_P.

$$U_M = U_K + U_P \tag{15.a}$$

In steady-state, the density of internal kinetic energy is constant, so is its volume integral over S.

$$\frac{dU_K}{dt} = 0 \tag{15.b}$$

$$\frac{dU_M}{dt} = \frac{dU_P}{dt} \tag{16}$$

Rewriting equation 13, using 14 and 15.c:

$$P \approx W_{MT} + W_{ET} + \frac{dU_P}{dt} \tag{17}$$

By expressing the three terms on the right, in terms of cutting process parameters, the above equation becomes an expression for the machine tool's power as a function of the process parameters. Table 1 lists the conversion mechanisms from U_E and U_M to U_T. The total rate of these mechanisms constitute W_{ET} and W_{MT}.

Source form	Mechanism of conversion to thermal
Electromagnetic	Joule Heating – Semiconductor dissipation
Mechanical	Dry friction – Viscous dissipation – Plastic deformation

Table 1. Energy conversion mechanisms within a typical CNC machine tool

3.3. Conversion of energy from mechanical to thermal; W_{MT}

Mechanical energy converts to thermal energy through three mechanisms: Dry friction, viscous dissipation and plastic deformation.

3.3.1. Dry friction

This occurs between solid surfaces in contact and relative motion at their contact. The dry friction force, F_{DF}, is proportional to N, the normal force between the two solids at their contact point, with the friction coefficient, μ, being the constant of proportionality. The rate of conversion of energy from mechanical to thermal through dry friction is, therefore:

$$\frac{dQ_{DF}}{dt} = \vec{F}_{DF} \cdot \vec{v} = \mu N v \tag{18}$$

where v is the relative velocity between the two objects at their contact. Dry friction in ancillary devices, e.g. the bearings of the lubricant pump, takes place at a constant rate, because N and v are constant and independent of the milling process parameter:

$$\left.\frac{dQ_{DF}}{dt}\right|_{ancil.} = C \tag{19}$$

At the contact of tool and workpiece, the normal force, N, is proportional to the MRR and v is proportional to the spindle speed, s. Therefore, the rate of conversion of energy from mechanical to thermal through dry friction mechanism at the tool tip is

$$\left.\frac{dQ_{DF}}{dt}\right|_{tool} = A(MRR)s \tag{20}$$

At the supports, bearings and drives of the machine bed, the normal forces are mainly determined by the weight of the bed, which is constant. However, to balance the force exerted on the workpiece by the tool tip, these normal forces change slightly by an additional term. The additional term is proportional to the tool tip force, because they result from the equilibrium equations, which are linear. The tool tip force is proportional to MRR. So, at the machine bearings:

$$N|_{bed.support} = A + B(MRR) \tag{21}$$

The relative velocity of surfaces in contact at the machine bed bearings are proportional to the feed rate, f. Therefore, the rate of conversion of energy from mechanical to thermal due to dry friction at the machine bed bearings is:

$$\left.\frac{dQ_{DF}}{dt}\right|_{bed.support} = (A + B(MRR))f \tag{22}$$

The above equation holds for every dry friction mechanism whose characteristic speed is proportional to feed rate. The same argument applies to the dry friction mechanisms whose speed is proportional to the spindle speed, e.g. in the spindle bearings, which will lead to:

$$\left.\frac{dQ_{DF}}{dt}\right|_{spindle.support} = (A + B(MRR))s \tag{23}$$

Combining equations 19, 20, 22 and 23, the total rate of conversion of energy from mechanical to thermal through dry friction may be written as:

$$\frac{dQ_{DF}}{dt} = C + \left(A_f + B_f(MRR)\right)f + \left(A_s + B_s(MRR)\right)s \tag{24}$$

3.3.2. Viscous dissipation

This occurs inside fluids with non-zero viscosity, wherever the strain rate tensor is non-zero. The form of relation between the rate of conversion and the characteristic velocity, v, is determined by the Reynolds number of the flow. For low Reynolds numbers, i.e. Stokes and other laminar flow, the viscous stresses are proportional to v, which result

in the rate of conversion of energy from mechanical to thermal being proportional to v^2. For large Reynolds numbers, i.e. fully developed turbulent flow, the viscous stresses are proportional to v^2, and therefore, the rate of dissipation is proportional to v^3. A typical example of these two regimes can be seen in Moody chart, for the flow in pipes.

The volumes occupied by fluids may be partitioned into low and high Reynolds number regions and the total rate of viscous dissipation may be found by adding the rates of all regions to find:

$$\frac{dQ_{VF}}{dt} = Dv^2 + Ev^3 \tag{25}$$

For the fluid flows whose speed are independent of the process parameters, e.g. flow of lubricant in pipes, the total rate of conversion remains constant, irrespective of the flow regime. For flows whose speed is determined by the spindle speed, e.g. air flow around the spindle, the characteristic speed, v, is proportional s, and for flows whose speed is determined by the feed rate, f, the characteristic speed is proportional to f. Therefore, for the total rate of conversion of energy from mechanical to thermal through viscous friction:

$$\frac{dQ_{VF}}{dt} = C + (D_f f^2 + E_f f^3) + (D_s s^2 + E_s s^3) \tag{26}$$

3.3.3. Plastic deformation

This mechanism occurs within a solid material undergoing plastic deformation. In a CNC machine tool, this happens during material removal, where plastic deformation continues until the material breaks. The amount of energy required to plastically deform a unit volume of a material until it breaks, is a property of the material, and almost independent of the process parameters. Therefore, the rate of conversion of energy from mechanical to thermal through plastic deformation is proportional to the rate of material removal, MRR:

$$\frac{dQ_{PD}}{dt} = K(MRR) \tag{27}$$

3.3.4. Total rate of conversion from mechanical to thermal

The total rate of conversion from mechanical to thermal, W_{MT} is the sum of the rates due to each of the three mechanisms above. Equations 28 is the result, in which, the terms are grouped into 4, according to their variables: a constant; a product of MRR

and a linear function of f and s; and two 3rd-order polynomials of f and s, both without constant terms.

$$W_{MT} = C + \left(K + B_f f + B_s s\right)(MRR) + \left(A_f f + D_f f^2 + E_f f^3\right) + \left(A_s s + D_s s^2 + E_s s^3\right) \quad (28)$$

3.4. Conversion of energy from electrical to thermal; W_{ET}

Conversion of energy from electromagnetic to thermal takes place through two different mechanisms in the machine's conductors and semiconductors. In semiconductors, e.g. in the machine's computers and, if present, semiconductor lightings, the potential difference across semi-conductor components is a constant and therefore, the rate of conversion of energy from electromagnetic to thermal is proportional to the current that passes through the component. However, since there is no relation between the cutting process and the activity of semiconductor components, the rate of this conversion is independent of the cutting parameters. In conductors, e.g. the main cable connecting the machine to the plug, the wiring in the machine's electromotors, eddy currents in the machine's transformers and electromotors, etc., the rate of energy conversion from electromagnetic to thermal is proportional to the square of current. In some conductors, the current, and therefore the rate of thermal dissipation, is independent of the cutting process, e.g. in lubricant pump electromotor.

However, in spindle motor and feed motors, the current depends on the cutting process and so does the rate of energy conversion from electromagnetic to thermal. In electromotors, the torque is proportional to the current:

$$\tau \propto I$$

As mentioned above, the rate of energy conversion from electromagnetic to thermal, P_{Res}, is proportional to the square of the current:

$$P_{Res} \propto \tau^2 \quad (29)$$

The torque, having to overcome dry friction, viscous friction and to contribute to material removal, obeys the

$$\tau_{sRes} = A' + B's + C's^2 + D'(MRR) \quad (30.a)$$
$$\tau_{fRes} = A" + B"f + C"f^2 + D"(MRR) \quad (30.b)$$

The total rate of direct energy conversion from electrical to thermal is:

$$W_{ET} = cte + \left(A' + B's + C's^2 + D'(MRR)\right)^2 + \left(A" + B"f + C"f^2 + D"(MRR)\right)^2 \quad (31)$$

3.5. Increase in internal potential energy, $\frac{dU_P}{dt}$

A fraction of the mechanical energy provided by the spindle motor at the tool tip, ends up stored in S in potential mechanical form as residual stress in cooled-down chips and workpiece. The rate of this increase is proportional to the rate of material volume going through this storage, which is proportional to the MRR.

$$\frac{dU_P}{dt} \propto MRR \quad (32)$$

as thermal and mechanical energy. enteres energy is being stored in potential mechanical form, as residual stress in the cooled-down chips and workpiece. The rate of this increase is proportional to the rate of material volume going through this storage, which is proportional to the MRR.

3.6. Total power consumption

Starting from equation 17 and replacing the three terms on its right side by their equivalents from equations 28, 31 and 32, equation 33 is constructed, which is a relationship between the machine tool's power P and the process parameters: f, s and MRR. The constants of similar terms of the constituent equations are combined to form the constants in equation 33.

$$P(f, s, MRR) = C + \left(A_f f + B_f f^2 + C_f f^3 + D_f f^4\right) + (A_s s + B_s s^2 + C_s s^3 + D_s s^4) + \left(E + F_f f + F_s s + G_s s^2 + G_f f^2\right)(MRR) + K(MRR^2) \quad (33)$$

Equation 33 is the final result of the model constructed above and provides a predictive equation for the power consumption of a milling machine during a cutting process, in terms of its feed rate, spindle speed and its rate of material removal.

4. Experimental validation of the model

To validate equation 33, a set of measurements is designed and made. The best fit of the equation 33 onto the collected data is found. The performance of the model is compared to some of the existing models. The results are also used to obtain a simpler form of the model by discarding the terms with small contributions to the total power consumption over the investigated domain of variables.

4.1. Equipment and material

The milling machine used for the experiment is a 3-axis Bridgeport VMC 610 XP[2]. The cutting tool chosen for the experiments is a 2-flute 14mm carbide end mill. The material is aluminium alloy 6082, which comes in identical blocks of size $230\times150\times37.5mm^3$.

The power measurement device used in the experiment is a "HIOKI 3169-20 Clamp on Power Hitester". Three HIOKI 9695-02 clamp-on sensors are also used along with the Hitester as current probes. The Hitester uses three direct connections to the machine's power supply wires for voltage measurements.

4.2. Domain of variables

Equation 33 expresses power in terms of three independent variables (s, f, MRR). It is possible to replace one of the variable with a function of these three terms without the independence of variables being compensated, if the determinant of the Jacobian matrix of the transformation is a nonzero real number. By replacing the MRR with the depth of cut, a, this condition is satisfied for nonzero values of feed, because:

$$MRR = fad$$

Where: d is the tool diameter.

$$a = \frac{MRR}{fd}$$

$$J = \frac{\partial(s, f, a)}{\partial(s, f, MRR)} = \begin{pmatrix} 1 & 0 & 0 \\ 0 & 1 & 0 \\ 0 & -\frac{MRR}{f^2 d} & \frac{1}{fd} \end{pmatrix}$$

$$\det(J) = \frac{1}{fd}$$

So we are allowed to replace the set of independent variables (s, f, MRR) with another set of independent variables (s, f, MRR), which is more convenient for design of experiments. There are constraints of different origins on the choice of cutting parameters, each making parts of the three-dimensional (s, f, a) space inaccessible. The nature of these constraints and the mathematical representation of the boundaries of the domain they define are discussed here.

4.2.1. Limitation on cutting speed

The cutting speed of materials should be within a certain range to achieve an acceptable cutting quality. Consulting with available machining guidelines, the range for cutting speed was chosen as:

$$75 \leq v_{(m/min)} \leq 175 \tag{34}$$

Using this range of cutting speeds and the diameter of the cutting tool being 14 mm, the range of spindle speed is found:

$$1705 < s < 3978$$

or roughly:

$$1700 < s_{(rpm)} < 4000 \tag{35}$$

4.2.2. Limitation on feed per tooth

The recommended range of chip load (feed per tooth) is:

$$0.15mm < C.L. < 0.25mm \tag{36}$$

In terms of cutting parameters, the above inequality may be written as:

$$0.3 < \frac{f_{(mm/min)}}{s_{(rpm)}} < 0.5 \tag{37}$$

4.2.3. Limitation on depth of cut

For cutting aluminium with the chosen 14mm end mill the upper limit of depth of cut is given to be 8mm. However, to keep the effect of tool wear at minimum, the maximum depth of cut was chosen to be 4mm. Hence:

$$a < 4mm \tag{38}$$

4.2.4. Limitation on machine tool power

The spindle motor of the CNC milling machine used for the experiments has a rated power of 13 kW. The maximum specific cutting energy for aluminium is 1.1 J/mm^3 (Dahmus and Gutowski, 2004). Therefore:

$$af \leq 5.0{\times}10^4 \, {mm^2}/{min} \tag{39}$$

4.2.5. Domain of cutting parameters

Constraints represented in equations 35, 37, 38 and 39 define a prismatic volume with trapezoidal base in the (s, f, a) space, as the accessible domain of cutting parameters. Figure 2 illustrates this domain.

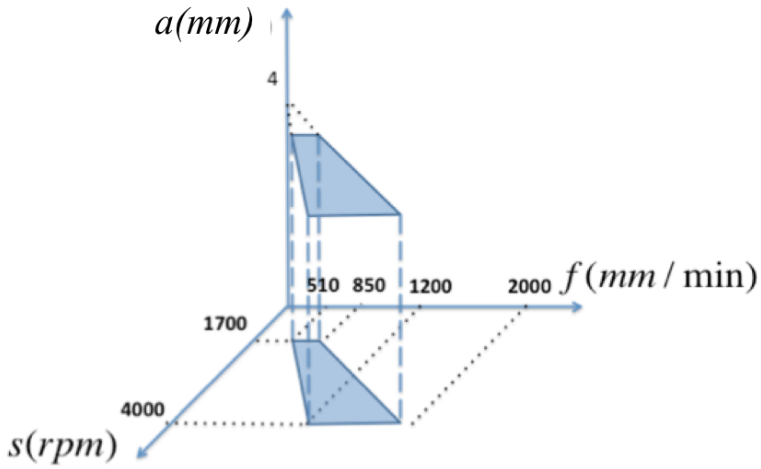

Figure 2. Accessible domain of cutting parameters

4.3. Design of experiment

The experiment has been designed such that:

- The entire domain is covered
- The domain in covered homogeneously, so the variations of power in all the domain is captured equally well
- The design is symmetric with respect to variables, so the data acquired can be equally used to test the accuracy of other models

A transformation was applied to transform the prismatic domain in (s, f, a) space to a unit cube in (σ, β, γ) space:

$$\begin{cases} s = 1700 + 2300\sigma \\ f = \left(\frac{\beta}{5} + 0.3\right)(1700 + 2300\sigma) \\ a = 4\gamma \end{cases} \quad (40)$$

This transformation is a nonlinear transformation and does not preserve the homogeneity of volumetric distribution of design points. Therefore, a homogeneous design in (s, f, a) space represents a nonhomogeneous design in (σ, β, γ) space and vice versa. Still, the authors argue that the homogeneity of the design should be

considered and applied in (σ, β, γ) space, where domain is a unit cube rather than (s, f, a) space, where it is a prismatic volume with trapezoidal base, mainly because this is the topology of the domain's boundaries that contains information about the physical causes of the shape of the domain not its geometry that is a construct in a 3-D Cartesian space based on three axes made of quantities with different physical dimensions. Also there exists a symmetric homogeneous design that covers the entire cube and that is an n^3 cubic design. It is also a simple design for an experimenter to follow and, therefore, reduces the risk of experimentation error. Therefore, an n^3 cubic design is chosen for this experiment.

Since in this model power consumption relates to feed and spindle speed through 3rd order polynomials and since any set of 4 or less data points (in 2-D speaking) can be fitted by a 3rd order polynomial, n should be no less than 5 or the experiment's ability to detect inconformity between the empirical data and the model's prediction would be questionable. $n > 5$ would be uneconomical as the number of measurement grows with n^3 and for $n = 5$ already 125 measurements have to be carried out. For $n = 6$ the figure would be more than 1.7 times larger at 216. Moreover, lower uncertainties are not achievable in the experiment because of an independent source of uncertainty, the imprecision of the measurement set up, which will be discussed quantitatively later. Hence:

$$n = 5 \tag{41}$$

σ, β and γ are then chosen from the set V.

$$V = \left\{0, \frac{1}{4}, \frac{1}{2}, \frac{3}{4}, 1\right\} \tag{42}$$

V^3 contains all 125 combinations of (σ, β, γ) and for each one of them, using (40), (s, f, a) can be calculated. For example, $(\sigma, \beta, \gamma) = \left(\frac{1}{4}, 0, \frac{1}{2}\right)$ refers to $(s, f, a) = \left(2275_{(rpm)}, 682_{(mm/min)}, 2_{(mm)}\right)$.

4.4. Data acquisition

A block of aluminium is installed on the machine bed with its long edge parallel to machine's x-axis. After face milling, 5 full-length longitudinal slots are cut on equally spaced paths, all at one certain combination of (σ, γ), i.e. (s, a). Each of the 5 slots is cut at a feed rate equivalent to a distinct β chosen from V. Slots are cut in the increasing feed rate order, i.e. increasing β from 0 to 1. This procedure is named a "measurement routine" by the authors and is repeated 25 times to cover all 125 combinations of (s, f, a).

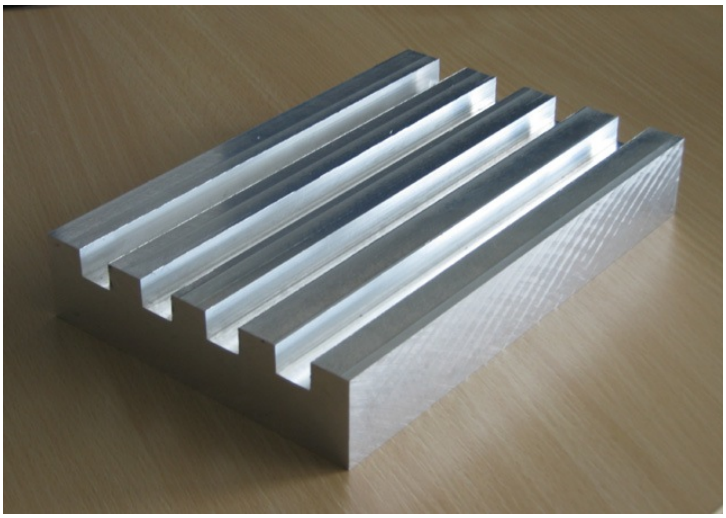

Figure 3. An aluminium block after a number of measurement routines (Newman et al., 2012)

The power measurement device records the apparent power, and some other related quantities, of the machine every one second during the time the slots are cut. Figure 4 shows a graph of the measured values of apparent power during the measurement routine run for $(\sigma, \gamma) = \left(\frac{1}{2}, \frac{3}{4}\right)$.

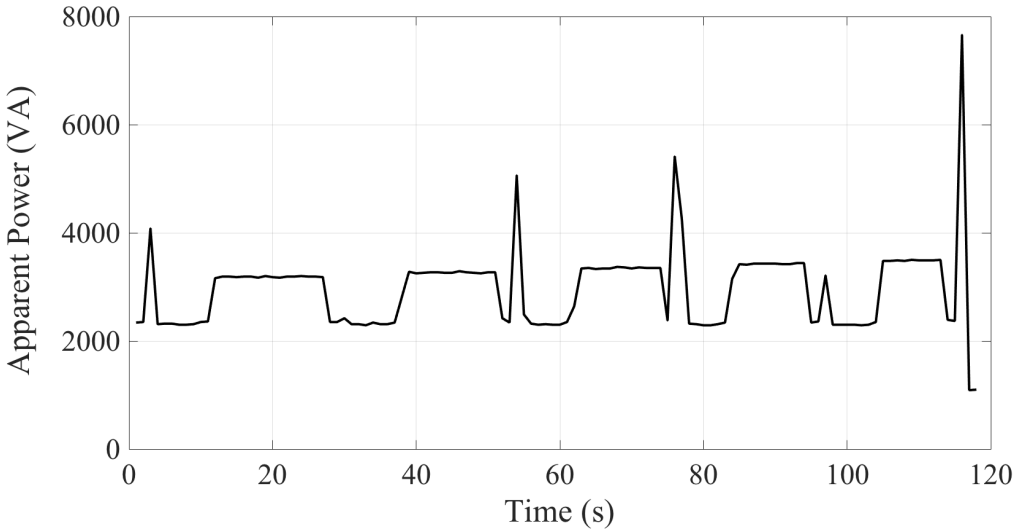

Figure 4. Apparent power readings during measurement routine for $(\sigma, \gamma) = \left(\frac{1}{2}, \frac{3}{4}\right)$

The five plateaus observed in figure 4 represent power readings during the slot cutting operations, which is the only part of the graph that is related to this research. The first plateau represents $\beta = 0$. β increases in steps of 0.25 to $\beta = 1$ for the 5th cut.

The average of recorded apparent powers for a plateau is defined as the measurement on machine's power consumption at the corresponding combination of (σ, β, γ).

Standard deviation of the same set of data is also calculated as a measure of random error. Ratio of standard deviation to the average is defined as the relative measurement error, η_{meas}. It was observed to be in the range:

$$\eta_{meas} = 0.30 \pm 0.05 \quad (43)$$

The result of application of this procedure to the set of data utilised to produce figure 4 is presented in table 2.

σ	γ	β	$\overline{P^E}(\alpha,\gamma,\beta)[V_A]$	$S(P^E)[V_A]$	$\eta_{meas} = \frac{S(P^E)}{(P^E)}[\%]$
0.5	0.75	0	3184	10	0.31
0.5	0.75	0.25	3266	9	0.27
0.5	0.75	0.5	3348	12	0.36
0.5	0.75	0.75	3426	11	0.32
0.5	0.75	1	3488	10	0.29

Table 2. Data extracted from the set of measurement routine presented in figure 4.

This data acquisition procedure is carried out 25 times, once for every combination of (σ,γ), hence 125 measurements. Face milling takes place only when the block is replaced with a new one. As long as the depth of slots is less than half the thickness of the block, cuts are made into the existing slots. The effect of wall friction is ignored.

4.5. uncertainty estimation

before the analysis of the acquired data, their uncertainties must be estimated.

4.5.1. Repetition tests

To evaluate the magnitude of the random error in the case of repetition of experiment, measurements were repeated 5 times for 8 of 125 combinations of (σ,β,γ), in a cubic 2^3 design containing corner points of the cube. The relative errors observed in repetition tests were in the range of 0.7 to 0.9%.

$$\eta_{rep} = 0.8 \pm 0.1 \quad (44)$$

4.5.2. Equipment accuracy

The measurement device's catalogue suggests that the accuracy in power readings may be found through equation (44) (Hioki, pp. 188).

$$S_{equip} = \pm 0.5\% rdg. \pm 0.14\% f.s. \quad (45)$$

In equation 45 "rdg." represents the reading value of power and "f.s." the full-scale power measurable by the combination of sensors and range selection used on the device during experiments, which is 60kVA. This introduces two independent uncertainties, one with constant relative magnitude: $\eta_{rdg} = 0.5\%$, and the other with constant absolute magnitude: $S_{f.s.} = 84(VA)$.

4.5.3. Overall uncertainty in observed values of apparent power

From the 4 error sources, η_{meas}, η_{rep}, η_{rdg} and $\eta_{f.s.}$, the last one dominates when estimating an overall uncertainty in the final measurement through:

$$S = \left[S_{meas}^2 + S_{rep}^2 + S_{rdg}^2 + S_{f.s.}^2\right]^{\frac{1}{2}} \quad (46)$$

to end up with values in the range:

$$S = 90 \pm 5(VA) \quad (47)$$

Which is an estimation of the uncertainty in each of 125 measurements of machine's apparent power consumption.

4.6. Data fitting and analysis

There are 15 terms on the right side of equation 33. Each term is made of the product of one unknown coefficient b_j and a function of the independent variables $g_j(s, f, a)$. Therefore, equation 33 may be written as:

$$P = \sum_{j=1}^{15} b_j g_j(f, h, s) \quad (48)$$

g_j functions and b_j coefficients are listed in table 3. The linear least square method was used to find the values of coefficients that provide the best fit to the 125 experimentally acquired power data. Table 4 contains the coefficients of the best fit. Figure 5 shows the distribution of residuals, i.e. the difference between predicted and measured power. The rms of residuals is:

$$\varepsilon_{rms} = 19VA \quad (49)$$

Since the uncertainty of measurements is 90VA, the empirical data does not falsify the model.

j	1	2	3	4	5	6	7	8	9	10	11	12	13	14	15
g_j	1	f	f^2	f^3	f^4	s	s^2	s^3	s^4	MRR	$fMRR$	$sMRR$	f^2MRR	s^2MRR	MRR^2
b_j	K	A_f	B_f	C_f	D_f	A_s	B_s	C_s	D_s	E	F_f	F_s	G_f	G_s	H

Table 3. List of g_j functions and b_j constants

j	Coeffecient
1	4.6681×10^{3}
2	-0.6189
3	8.6705×10^{-4}
4	-4.5086×10^{-7}
5	8.2315×10^{-11}
6	-2.9120
7	0.0014
8	-3.1646×10^{-7}
9	2.5796×10^{-11}
10	0.0279
11	-1.7269×10^{-5}
12	3.0910×10^{-6}
13	3.1361×10^{-9}
14	-2.2890×10^{-10}
15	2.9619×10^{-8}

Table 4. Coefficients of the best fit according to the linear least square method

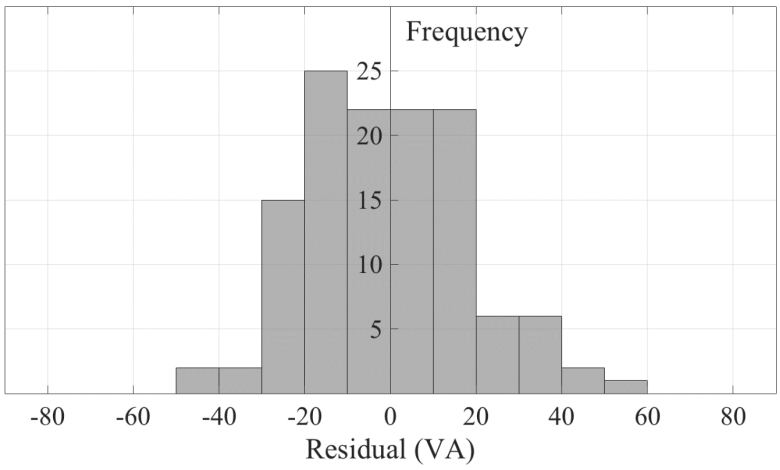

Figure 5. Distribution of residuals.

5. Discussion

This consists of four major areas; model comparison, simplified form of the model and, critique of the analysis and application of the constructed model.

5.1. Comparison with other models

The power measures acquired during the experiment may also be used to assess the performance of other existing models of energy consumption in machining. This has been carried out for two widely used models proposed by Gutowski et al. (2006) and Li et al. (2013), i.e. equations 2 and 3 respectively. These two models are both truncated forms of the model proposed in this paper. Applying the same linear regression method, the best fits of the two models to the acquired data was found. The rms of residuals are 75VA for equation 2 model and 68VA for equation 3 model. Equation 3, despite having one more term than equation 2, only has a marginally better performance than that. The proposed model in this paper, with 19VA rms of residuals, has a significantly better performance than both analysed models. The rms of relative errors, i.e. errors divided by corresponding measured powers, is %0.67, in contrast with %2.28 for equation 2 and %2.05 for equation 3.

5.2. A Simplified form of the model

After observation of the good performance of equation 2, despite having only two terms, and the marginal improvement that the additional term in equation 3 provides, it was decided to analyse the performance of all 3-term truncated forms of equation 32. The number of possible 3-term combinations of the 15 terms of equation 32 is $\binom{15}{3} = 455$. All 455 were fitted to the experimental data and rms of their residuals were calculated. Figure 6 shows the distribution of the calculated rms values.

The smallest rms is 42VA and corresponds to the combination of the 1st, 10th and 11th terms. Therefore, the most precise 3-term truncated form of equation 32, with rms as small as twice as that of the complete 15-term model is:

$$P(f, s, MRR) = C + E(MRR) + F_f f(MRR) \qquad (50)$$

Interestingly, from all 455 combinations, only the 13 combinations that contain both terms of equation 2 have rms smaller than that of equation 2, i.e. 75VA, which confirms the high accuracy of equation 2, despite being a simple 2-term model.

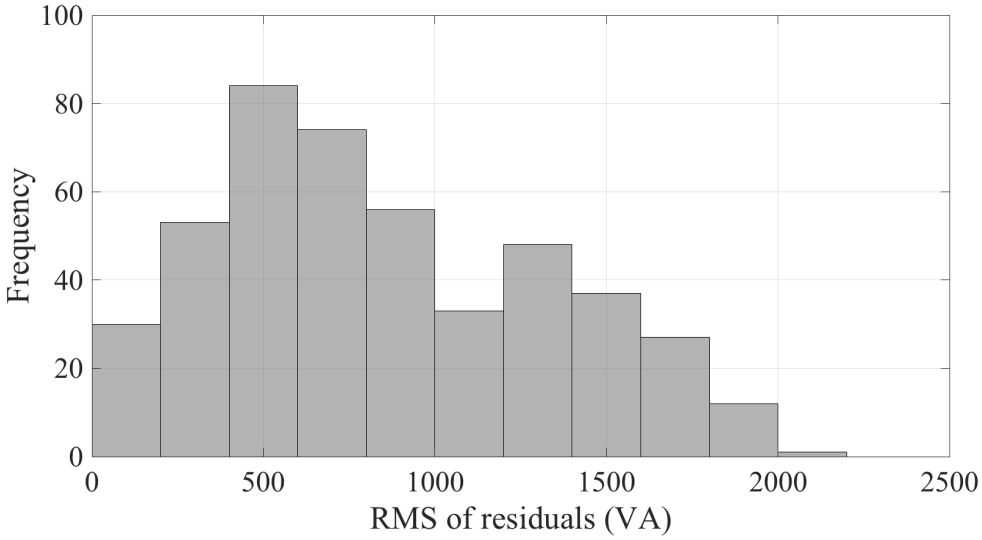

Figure 6. Distribution of 455 rms of residuals for 3-term truncated forms of eq. 32

5.3. Critique of the analysis

The uncertainty in measurements made during the experiments has been 90VA. As this is larger than the observed rms of residuals of the best fit of both the proposed model, i.e. 19VA, and that of the other two models described by equations 2 and 3, i.e. 75VA and 68VA, the conducted experiment cannot falsify any of the models. More accurate measurements, with uncertainty of order of magnitude of no more than 10VA are required to fundamentally distinguish between the performances of the proposed model and other existing ones.

The power rating of the CNC machine used in the experiments is 13kW, but the measured powers during the experiments have all been within the [2.3,4.5]kW. Since the share of non-linear terms in the model grow by the total power, to better capture their effect, further experiments should be conducted at higher powers.

Fitting the model to the experimentally acquired data using the least square method results in both positive and negative coefficients, visible in figure 5. However, because each of the 15 terms of equation 32 represents a rate of conversion, or the collection of a few of them, it is expected for the coefficients to be positive. The only exception might be the effect of balancing forces at machine bearings that are results of equilibrium equations and may be large enough to produce negative coefficients. Therefore, trying a non-negative least square method could, potentially, produce more realistic coefficients with more meaningful terms. This remains to be investigated

further in future. Further experiments with other machines, tools and workpiece materials are required to test the generality of the model proposed in this work.

5.4. Application of the model

The constructed model can also be utilised in process planning to choose milling process parameters in order to either minimise the total consumed energy during the process, as a single objective optimisation problem, or to reach an optimum combination of a number of objective parameters, including the total consumed energy. There would be no intrinsic difference between the model constructed in this paper and other existing models in the way they may be used to achieve the aforementioned goals, but the higher accuracy of this model will lead to more accurate choice of process parameters and lower total energy consumption.

6. Conclusions

A mechanistic model of energy flow through a CNC machine tool performing a steady-state slot milling was constructed through mapping of energy conversions inside the machine tool as a thermodynamic system, figure 1. The model leads to equation 33 that expresses power consumption of the machine tool as a function of spindle speed, feed rate and the rate of material removal (s, f, MRR).

Equation 33 was validated experimentally on a 3-axis CNC milling machine, Bridgeport VMC 610 XP^2, cutting Al6082, using a 14mm 2-flute end mill. The model was found superior more than three times more accurate than two other existing models: Gutowski et al. (2006) and Li et al. (2013), i.e. equations 2 and 3 respectively.

The best fitting 3-term truncated form of equation 33 to the experimental data was found, among 455 possible combinations, which is given in equation 50. It provides a simple, yet accurate estimation of the machine's power consumption, within the range of process parameters investigated in the experiment. Further investigation of the proposed model, with more accurate measurements on a variety of machines, cutting tools and workpiece material, over a larger range of machine power and application of non-negative least square data fitting can increase the robustness of the model.

The model constructed in this paper provides an accurate, simple and powerful tool to enable companies that use machining technologies to accurately predict and minimise

their energy consumption at machine and factory levels. This will lead to significant cost savings and reduction of environmental impact for such companies.

.

References

Akbari, J., Oyamada, K. and Saito, Y., 2001. LCA of machine tools with regard to their secondary effects on quality of machined parts. In *Environmentally Conscious Design and Inverse Manufacturing, 2001. Proceedings EcoDesign 2001: Second International Symposium on* (pp. 347-352). IEEE.

Balogun, V.A. and Mativenga, P.T., 2013. Modelling of direct energy requirements in mechanical machining processes. *Journal of Cleaner Production*, *41*, pp.179-186.

Bruzzone, A.A.G., Anghinolfi, D., Paolucci, M. and Tonelli, F., 2012. Energy-aware scheduling for improving manufacturing process sustainability: A mathematical model for flexible flow shops. *CIRP Annals-Manufacturing Technology*, *61*(1), pp.459-462.

Cai, W., Liu, F., Xie, J., Liu, P. and Tuo, J., 2017. A tool for assessing the energy demand and efficiency of machining systems: Energy benchmarking. *Energy*, *138*, pp.332-347.

Camposeco-Negrete, C., 2013. Optimization of cutting parameters for minimizing energy consumption in turning of AISI 6061 T6 using Taguchi methodology and ANOVA. *Journal of Cleaner Production*, *53*, pp.195-203.

Dahmus, J.B. and Gutowski, T.G., 2004, November. An environmental analysis of machining. In *ASME international mechanical engineering congress and RD&D expo* (pp. 13-19).

De Filippi, A., Ippolito, R. and Micheletti, G.F., 1981. NC machine tools as electric energy users. *CIRP Annals-Manufacturing Technology*, *30*(1), pp.323-326.

Department for Business, Energy & Industrial Strategy, UK Government, 2017a. *Energy Consumption in the UK*.

Department for Business, Energy & Industrial Strategy, UK Government, 2017b. *Energy Consumption in the UK (ECUK) Data Tables*. [Online]. [Accessed 14 August 2017]. Available from: https://www.gov.uk/government/statistics/energy-consumption-in-the-uk

Diaz, N., Redelsheimer, E. and Dornfeld, D., 2011. Energy consumption characterization and reduction strategies for milling machine tool use. *Glocalized solutions for sustainability in manufacturing*, pp.263-267.

Draganescu, F., Gheorghe, M. and Doicin, C.V., 2003. Models of machine tool efficiency and specific consumed energy. *Journal of Materials Processing Technology*, *141*(1), pp.9-15.

Draganescu, F., Gheorghe, M. and Doicin, C.V., 2003. Models of machine tool efficiency and specific consumed energy. *Journal of Materials Processing Technology*, *141*(1), pp.9-15.

Duflou, J.R., Sutherland, J.W., Dornfeld, D., Herrmann, C., Jeswiet, J., Kara, S., Hauschild, M. and Kellens, K., 2012. Towards energy and resource efficient manufacturing: A processes and systems approach. *CIRP Annals-Manufacturing Technology*, *61*(2), pp.587-609.

Guo, Y., Loenders, J., Duflou, J. and Lauwers, B., 2012. Optimization of energy consumption and surface quality in finish turning. *Procedia CIRP*, *1*, pp.512-517.

Gutowski, T., Dahmus, J. and Thiriez, A., 2006, May. Electrical energy requirements for manufacturing processes. In *13th CIRP international conference on life cycle engineering* (Vol. 31, pp. 623-638).

Hu, L., Peng, C., Evans, S., Peng, T., Liu, Y., Tang, R. and Tiwari, A., 2017. Minimising the machining energy consumption of a machine tool by sequencing the features of a part. *Energy*, *121*, pp.292-305.

Hu, L., Tang, R., He, K. and Jia, S., 2015. Estimating machining-related energy consumption of parts at the design phase based on feature technology. *International Journal of Production Research*, *53*(23), pp.7016-7033.

Imani Asrai, R., Newman, S. and Nassehi, A., 2009. A power consumption model for slot generation with a CNC milling machine. In *19th International Conference on Flexible Automation and Intelligent Manufacturing (FAIM)* (pp. 955-963). University of Bath.

Imani Asrai, R., 2013. *Mechanistic modelling of energy consumption in CNC machining* (Doctoral dissertation, University of Bath).

International Energy Agency, 2016. *World Energy Outlook*. OECD, Paris.

Jeon, H.W., Lee, S., Kargarian, A. and Kang, Y., 2017. Power demand risk models on milling machines. *Journal of Cleaner Production*, *165*, pp.1215-1228.

Kara, S. and Li, W., 2011. Unit process energy consumption models for material removal processes. *CIRP Annals-Manufacturing Technology*, *60*(1), pp.37-40.

Kishawy, H.A., Kannan, S. and Balazinski, M., 2004. An energy based analytical force model for orthogonal cutting of metal matrix composites. *CIRP Annals-Manufacturing Technology*, *53*(1), pp.91-94.

Li, W. and Kara, S., 2011. An empirical model for predicting energy consumption of manufacturing processes: a case of turning process. *Proceedings of the Institution of Mechanical Engineers, Part B: Journal of Engineering Manufacture*, *225*(9), pp.1636-1646.

Li, Y., He, Y., Wang, Y., Yan, P. and Liu, X., 2014. A framework for characterising energy consumption of machining manufacturing systems. *International Journal of Production Research*, *52*(2), pp.314-325.

Lund, H., 2007. Renewable energy strategies for sustainable development. *Energy* 32(6), pp.912-919.

Mori, M., Fujishima, M., Inamasu, Y. and Oda, Y., 2011. A study on energy efficiency improvement for machine tools. *CIRP Annals-Manufacturing Technology*, *60*(1), pp.145-148.

Mouzon, G., Yildirim, M.B. and Twomey, J., 2007. Operational methods for minimization of energy consumption of manufacturing equipment. *International Journal of Production Research*, *45*(18-19), pp.4247-4271.

Munoz, A.A. and Sheng, P., 1995. An analytical approach for determining the environmental impact of machining processes. *Journal of materials processing technology*, *53*(3-4), pp.736-758.

Newman, S.T., Nassehi, A., Imani-Asrai, R. and Dhokia, V., 2012. Energy efficient process planning for CNC machining. *CIRP Journal of Manufacturing Science and Technology*, *5*(2), pp.127-136.

Prabhu, V.V., Trentesaux, D. and Taisch, M., 2015. Energy-aware manufacturing operations. *International Journal of Production Research*, 53(23), pp.6994-7004.

Rajemi, M.F., Mativenga, P.T. and Aramcharoen, A., 2010. Sustainable machining: selection of optimum turning conditions based on minimum energy considerations. *Journal of Cleaner Production*, *18*(10), pp.1059-1065.

Schudeleit, T., Züst, S. and Wegener, K., 2015. Methods for evaluation of energy efficiency of machine tools. *Energy*, *93*, pp.1964-1970.

Schudeleit, T., Züst, S., Weiss, L. and Wegener, K., 2016. The total energy efficiency index for machine tools. *Energy*, *102*, pp.682-693.

Shin, S.J., Suh, S.H. and Stroud, I., 2015. A green productivity based process planning system for a machining process. *International Journal of Production Research*, *53*(17), pp.5085-5105.

Su, W., Xie, X., Li, J., Zheng, L. and Feng, S.C., 2017. Reducing energy consumption in serial production lines with Bernoulli reliability machines. *International Journal of Production Research*, pp.1-24.

US Energy Information Administration, US Department of Energy, 2016. *International Energy Outlook 2016 with projections to 2040*

Wang, L., Wang, W. and Liu, D., 2017. Dynamic feature based adaptive process planning for energy-efficient NC machining. *CIRP Annals-Manufacturing Technology*.

Xie, J., Liu, F. and Qiu, H., 2016. An integrated model for predicting the specific energy consumption of manufacturing processes. *The International Journal of Advanced Manufacturing Technology*, *85*(5-8), pp.1339-1346.

Yoon, H.S., Lee, J.Y., Kim, H.S., Kim, M.S., Kim, E.S., Shin, Y.J., Chu, W.S. and Ahn, S.H., 2014. A comparison of energy consumption in bulk forming, subtractive, and additive processes: Review and case study. *International Journal of Precision Engineering and Manufacturing-Green Technology*, *1*(3), pp.261-279.

Zolgharni, M., Jones, B.J., Bulpett, R., Anson, A.W. and Franks, J., 2008. Energy efficiency improvements in dry drilling with optimised diamond-like carbon coatings. *Diamond and Related Materials*, *17*(7), pp.1733-1737